On the Enhanced X-ray Emission From SGR 1900+14 after the August 27^{th} Giant Flare

Ü. Ertan[1] and M. A. Alpar[2]

Sabancı University, Orhanlı– Tuzla 34956 İstanbul/ Turkey

ABSTRACT

We show that the giant flares of soft gamma ray repeaters ($E \sim 10^{44}$ erg) can push the inner regions of a fall-back disk out to larger radii by radiation pressure, while matter remains bound to the system for plausible parameters. The subsequent relaxation of this pushed-back matter can account for the observed enhanced X-ray emission after the August 27^{th} giant flare of SGR 1900+14. Based on the results of our models, we estimate that the ratio of the fluences of the enhanced X-ray emissions to that of the preceding bursts remains constant for a particular SGR with similar pre burst inner disk conditions, which is consistent with the four different burst observations of SGR 1900+14.

Subject headings: pulsars: individual (SGR 1900+14) — stars: neutron — X-rays: bursts — accretion, accretion disks

1. Introduction

Soft gamma ray repeaters (SGRs) are neutron stars that emit short ($\lesssim 1$ s) and luminous ($\lesssim 10^{42}$ erg s^{-1}) soft gamma ray bursts in their active phases. The burst repetition time scales extend from a second to years (see Hurley 2000 for a review). In their quiescent states, they emit persistent X-rays at luminosities similar to those of anomalous X-ray pulsars (AXPs) ($L \sim 10^{34} - 10^{36}$ erg s^{-1}). The spin periods of both SGRs and AXPs are in a remarkably narrow range ($P \sim 5$ - 12 s) (see Mereghetti 2000 for a review of AXPs). Four SGRs (and one candidate) and six AXPs are known up to date. Some of them were reported to be associated with supernova remnants indicating that they are young objects. Recently, some AXPs also showed bursts similar to those of SGRs, which probably imply that they belong to the same class of objects.

[1]unal@sabanciuniv.edu

[2]alpar@sabanciuniv.edu

Over the burst history of SGRs, two giant flares were exhibited by SGR 0526-66 (Mazets et al. 1979) and SGR 1900+14 (Hurley et al. 1999). These giant flares are characterized by an initial hard spike with a peak luminosity $\sim 10^{44} - 10^{45}$ erg s^{-1} which lasts a fraction of a second. The hard spike is followed by an oscillating tail that decays in a few minutes. Assuming isotropic emission the fluence of the entire giant flare is about $\sim 10^{44}$ ergs (Hurley et al. 1999; Feroci et al. 2001; Mazets et al. 1999).

Magnetar models can explain the super-Eddington luminosities of the normal and the giant bursts of SGRs by the sudden release of the very high magnetic energies from inside the neutron stars (Thompson & Duncan 1995). In an alternative class of models, fall-back disks around young neutron stars can account for the period evolution of these systems, and in particular for the period clustering of SGRs and AXPs (Chatterjee, Hernquist, & Narayan 2000; Alpar 2001). Thompson et al. (2000) argued that the high luminosity of a giant flare would excavate any accretion disk to a large radius (due to the radiation momentum) and rebuilding of the entire disk takes months to years; so that the enhancement and the decay of the persistent X-ray flux after the giant flare could not be related to any disk accretion phenomenon.

The persistent X-ray emission from SGR 1900+14 was reported to increase by a factor ~ 700 about 1000 s after the giant flare. The subsequent decay is a power law with an index ~ 0.7 (Woods et al. 2001). This increase and decay in the persistent X-ray emission of the SGR 1900+14 is our main interest here. It was proposed that the enhanced X-ray emission is due to the cooling of the neutron star crust after being heated by the energy of the giant flare (Lyubarsky, Eichler, & Thompson 2002). Here we show by means of a numerical disk model that (*i*) the X-ray enhancement can be explained in terms of the viscous relaxation of a disk pushed back by the giant flare, (*ii*) the amount of disk matter pushed out while remaining bound corresponds to a plausible fraction of the flare energy. The origin of the giant flare, which is probably the release of the high magnetic energy inside the NS by an instability, is not addressed in our model.

In the next section, we summarize the X-ray observations of SGR 1900+14 revealing the large flux changes in the persistent X-ray emission following the August 27 giant flare. In Sec.3, we present the details of the numerical disk models. The results of the model fits are discussed in Sec. 4. The conclusions are summarized in Sec. 5.

2. The X-Ray Data

The X-ray (2-10 keV) flux data following the August 27 giant flare of SGR 1900+14 shown in Figures 1-3 was taken from Woods et al. (2001). The first and the second data points (filled squares) are from RXTE/ASM measurements, and correspond to ~ 24 minutes and ~ 2 hours after the giant flare (Remillard et al. 1998; see Woods et al. 2001 for the measurements and the associated uncertainties). The two data points about 20 days after the giant flare are from the net source intensity measurements of BeppoSAX (filled triangle) and ASCA (filled circle) satellites. The remaining data points (crosses) are estimated from the pulsed intensity measurements by RXTE/PCA (Woods et al. 2001) as follows. Four BeppoSAX NFI observations of SGR 1900+14 (2000 March/April, 1998 September, and 1997 May) give similar pulsed fractions (~ 0.1) despite the varying intensity, pulse profile, and burst activity. In the light of these observations, Woods et al.(2001) estimated the total source intensity from the pulsed intensity measurements by assuming a constant pulsed fraction ($\mathcal{F}_{\rm rms} \sim 0.11$). There is a good agreement between these estimates, and the BeppoSAX and ASCA source intensity measurements about 20 days after the giant flare (see Woods et al. 2001 for more details). The reported relative pulsed fraction changes along the X-ray tails following the other observed bursts of SGR 1900+14 do not exceed a factor ~ 2 in the extreme case (Lenters et al. 2003). This does not affect the quality of our fits, but might require a small modification of the model parameters presented here. Keeping these uncertainties in mind we adopt for our numerical model the X-ray data set shown in Figures 1-3, obtained by scaling with the pulsed fraction $\mathcal{F} = 0.1$ where only the pulsed signal is observed.

3. The Numerical Model

Assuming isotropic emission, the total emitted energy during the giant flare is $\sim 10^{44}$ ergs (Mazets et al. 1999). A fraction of this emission is expected to be absorbed by the disk depending on the solid angle provided by the disk for the isotropic emission. For such a point-like emission at the center of the disk, the radiation pressure is expected to affect mostly the inner regions of the disk by pushing the inner disk matter to larger radii depending on the energy imparted to the disk matter. This leads to large density gradients at the inner rim of the disk immediately after the giant flare. We test whether the consequent viscous evolution of the disk can reproduce the X-ray flux data, consistently with the reported energy arguments of the giant flare.

In our model, we represent pushed-back inner disk matter, which we assumed to be formed by the radiation pressure of the giant flare, by a Gaussian surface density distribution

$\Sigma(R, t=0) = \Sigma_{\rm max}\ exp\left[-\left(\frac{R-R_0}{\Delta R}\right)^2\right]$, representing the pile up, added to the inner edge, at R_0, of the extended disk profile for which we chose the form $\Sigma = \Sigma_0(R_0/R)$. Σ_0 is a constant much less than $\Sigma_{\rm max}$, R is the radial distance from the center of the disk, and R_0 is the initial radial position of the center of the Gaussian. This form of the extended disk is close to the surface density profile of a standard thin disk (Shakura & Sunyaev 1973). In addition to the post-flare radius R_0, Σ_0, the Gaussian width and the maximum initial surface density $\Sigma_{\rm max}$ (at the center of the Gaussian) are the free parameters of our model. The disk's inner radius $R_{\rm in}$ (where the subsequent inflow of the pushed-back matter will be stopped by the magnetic pressure), and the outer disk radius $R_{\rm out}$ are kept constant throughout the calculations. A constant outer disk radius was chosen due to numerical reasons. Outer disk properties can only affect the inflow rate through the inner disk after several weeks or more in the absence of large surface density gradients at the outer disk regions. We use the one dimensional disk code described in Ertan & Alpar (2002), originally constructed to simulate the black hole soft X-ray transient accretion disks in outburst.

For a Keplerian thin disk the mass and angular momentum conservation equations give a non-linear diffusion equation for the surface density

$$\frac{\partial \Sigma}{\partial t} = \frac{3}{R}\frac{\partial}{\partial R}\left[R^{1/2}\frac{\partial}{\partial R}(\nu \Sigma R^{1/2})\right] \tag{1}$$

(Frank et al. 1992), where ν is the kinematic viscosity which, together with the surface densities, can be related to the disk midplane temperatures $T_{\rm c}$ through

$$\frac{4\sigma}{3\tau}T_{\rm c}^4 = \frac{9}{8}\nu\Sigma. \tag{2}$$

$\tau = \kappa\Sigma$ is the vertically integrated optical depth, and σ is the Stefan-Boltzmann constant. For the viscosity we use the standard α prescription $\nu = \alpha c_{\rm s} h$ (Shakura & Sunyaev 1973) where $c_{\rm s} = kT_{\rm c}/\mu m_{\rm p}$ is the local sound speed, μ the mean molecular weight, $h = c_{\rm s}/\Omega_{\rm K}$ the pressure scale height of the disk, and $\Omega_{\rm K}$ the local Keplerian angular velocity of the disk. We use electron scattering opacities ($\kappa_{\rm es} \simeq 0.4$ cm^2 g^{-1}). We chose $\mu = 0.6$ and $\alpha = 0.1$ which is typical of the hot state viscosities in the disk models of dwarf novae and soft X-ray transients.

By setting $x = 2R^{1/2}$ and $S = x\Sigma$, Eq.(1) can be written in a simple form

$$\frac{\partial S}{\partial t} = \frac{12}{x^2}\frac{\partial^2}{\partial x^2}(\nu S). \tag{3}$$

We divide the disk into 400 equally spaced grid points in x. This provides a better spatial resolution for the inner disk in comparison to a model with the same number of grid points equally spaced in R.

For a thin disk, the total disk luminosity is $L_{\rm disk} = GM\dot{M}_{\rm in}/2R_{\rm in}$, and most of this emission comes from the inner disk, characterized by a disk black-body spectrum. Here, $\dot{M}_{\rm in}$ is the mass inflow rate arriving at the disk inner radius $R_{\rm in}$, and M is the mass of the neutron star (NS). We take $M = 1.4M_{\odot}$ throughout the calculations. The accretion luminosity from the NS surface, $L_* = GM\dot{M}_*/R_*$, determines the observed luminosity in the X-ray band. The evolution of $\dot{M}_{\rm in}(t)$ in the disk will be reflected in the accretion luminosity from the NS surface, depending on the fraction of matter accreted, $f = \dot{M}_*/\dot{M}_{\rm in}$ where $\dot{M}_*$ is the mass accretion rate onto the star. We present three model calculations corresponding to different f values (0.1, 0.5, 0.9).

While the observed luminosity is expected to be powered by accretion onto the NS surface, the spectra during the enhanced X-ray emission of SGR 1900+14 can be fitted by a single power-law (Woods et al. 2001). A scattering source, e.g. a hot corona, around the inner disk can significantly change the spectrum emitted from the neutron star surface and from the disk black-body spectrum into a power-law spectrum by means of inverse Compton scatterings. If the source of the corona is fed by the thermal instabilities at the surface (or inner rim) of the disk then the total luminosity remains constant for a given matter inflow rate and inner disk radius, while the spectrum may be modified from the input spectrum. Comparison of spectral models for emission from the NS surface or the disk with the observed $2-10$ keV band data may be misleading. We take the observed luminosity to represent the total luminosity assuming that most of the X-ray flux from the source is emitted in the observation band (2-10 keV). For the model fits, we relate the model luminosities to the fluxes by $F_{\rm disk} \sim (L_{\rm disk}\ cos\ i)/(4\pi d^2)$ and $F_* \sim L_*/(4\pi d^2)$ where $d = 14.5$ kpc is the distance of the source (Vrba et al. 2000). We set $cos\ i = 0.8$ and neglected the small time delay for the matter to travel from $R_{\rm in}$ to R_*.

4. Results and Discussion

The disk parameters for the model curves presented in Figures 1-3 are given in Table 1. The lower and the upper model curves in the Figures correspond to the fluxes originating from the inner disk and from the NS surface respectively with $L_* = 2(\dot{M}_*/R_*)(R_{\rm in}/\dot{M}_{\rm in})L_{\rm disk} = 2f(R_{\rm in}/R_*)L_{\rm disk}$. For each of the three different f values (0.1, 0.5, 0.9) $L_x >> L_{\rm disk}$. Our models produce good fits to the wide range of f. For each mass accretion ratio f, the quiescent luminosity gives the mass inflow rate in the disk. The $R_{\rm in}$ values given in Table 1 are estimated Alfvén radii for these mass inflow rates, taking the dipole magnetic moment $\mu = 10^{30}$ G cm^3. These results strongly suggest a viscously evolving disk origin for the observed post burst X-ray enhancement, but do not constrain f. In this range of f, rough

estimates with the thin disk model give $m_I \simeq 19 - 20.5$ at the peak of the light curve, and $m_I \simeq 26$, similar to the upper limits in the quiescent phase (Vrba et al, 2000). The upper limits placed by the IR observations about 8 days after the giant flare, when the X-ray flux has decreased to about one percent of its peak level, are $m_J \gtrsim 22.8$ and $m_{K_s} \gtrsim 20.8$ (Kaplan et al. 2002). The IR expected light curve during the X-ray enhancement and in quiescence will be presented in a separate work.

The energy given to the disk by the giant flare could be written as $\delta E = \beta \dot{E} \Delta t \sim \beta 10^{44}$ ergs where $\beta = \beta_{\rm b} + \beta_{\rm e}$ is the fraction of the total flare energy absorbed by the disk. Part of the inner disk matter heated by the energy $\beta_{\rm e}\delta E$ can escape from the system, while the remaining part is pushed back by $\beta_{\rm b}\delta E$ staying bound and piling up at the inner rim of the disk. β is expected to be around $\sim 2\pi(2H_{\rm in})R_{\rm in}/4\pi R_{\rm in}^2 = H_{\rm in}/R_{\rm in} \sim$ few $\times 10^{-3}$ for a thin disk with $\dot{M} \sim 10^{15-16}$ g s^{-1} where $H_{\rm in}$ is the semi-thickness of the disk at $R_{\rm in}$. This ratio is roughly constant throughout the disk (e.g. Frank et al. 1992). The energy imparted by the flare to push back the inner disk matter is: $\delta E_{\rm b} \simeq (GM\delta M/2R_{\rm in})[1 - (R_{\rm in}/R_0)]$. This is almost equal to the binding energy, since we find that $R_{\rm in}/R_0 \sim 1/3$ for the models given in Table 1. The energy used up pushing back the disk is a fraction of the estimated energy, absorbed by the disk, $\beta_{\rm b} < \beta$. It is in fact likely that a larger amount of matter escapes from the system, than the amount δM that is pushed back but remains bound, with $\beta_{\rm e} \sim (5 - 25)\beta_{\rm b}$.

The maximum amount of mass that can escape from the inner disk during a burst can be estimated as $\delta M_{\rm loss} \sim (2R_{\rm in}/GM)\beta\delta E \simeq 10^{23}$ g $R_{\rm in,8}$ $(\beta/10^{-3})$ where $R_{\rm in,8}$ is the inner disk radius in units of 10^8 cm. During the lifetime of an SGR ($\sim 10^4$ yrs) which has a giant burst per century, the total mass loss would be 10^{25} g $R_{\rm in,8}$ $(\beta/10^{-3})$.

If the pulsed fraction remains the same (~ 0.1) throughout the enhanced X-ray flux phase as estimated by Woods at al. (2001) we expect a connection between the mass inflow rate and the pulsed X-ray emission. In our models, the luminosity from the NS surface dominates the disk luminosity, and the pulsed fraction $\mathcal{F} \sim 0.1$ could be explained as the ratio of the emission beamed by the mass flow geometry through the polar caps to the isotropic emission from or near the NS surface.

The time evolution in our models is quite prompt, with a viscous time scale $t_\nu \sim R^2/\nu \sim 10^3$ s, in agreement with the observed X-ray enhancement. Thompson et al. (2000) estimate a viscous time scale of ~ 10 yrs for the reestablishment of the inner disk mainly because they use pre burst mass flow rate $\dot{M} \simeq 10^{15}$ g s^{-1} in their estimate, instead of the appropriate post burst $\dot{M}$, which is three orders of magnitude higher. Thompson et al. also take $\alpha = 0.01$ and estimate the post burst inner disk radius to be $R_0 = 10^{10}$ cm. In our calculations, $\alpha = 0.1$, typical of the outburst (hot) states of the soft X-ray transient and dwarf nova disk models.

The post burst pile up position $R_0 \sim 10^9$ cm in our models corresponds to the short viscous time scale. For smaller burst energies (10^{41-42} ergs), the inner disk matter is pushed out to correspondingly smaller radii R_0, and t_ν could be as small as a few seconds.

The enhanced mass inflow rate can modify the spin evolution significantly especially around the peak of the X-ray light curve when $L_{\rm X}$ is about ~ 700 times higher than its quiescent level. A similar increase in $\dot{M}_{\rm in}$ corresponds to a decrease in the Alfvén radius $r_{\rm A}$ by a factor ~ 6 (or less if the field lines are compressed by rapid accretion). If the fastness parameter $\omega = \Omega_*/\Omega_{\rm K}(r_{\rm A})$ drops below unity a spin up is expected to prevail until ω has reduced back. If the system does not enter the spin-up phase or remains mostly in the spin-down phase in the high mass inflow regime, a sharp increase in the spin down torque could abruptly reduce the spin frequency. The changes in the spin evolution depends not only on the variations of the $\dot{M}_{\rm in}$ and ω but also on how close the system is to rotational equilibrium in quiescence and on the inner disk structure (likely to be somewhat different from a thin disk geometry) during the X-ray enhancement phase. Due to these uncertainties it is hard to make a reliable estimate of the spin evolution during the short term unsteady phase of these systems. A detailed examination of the possible post-burst spin evolution considering different accretion geometries will be addressed in future work.

Observations of four bursts from SGR 1900+14, including the August 27 giant flare and 3 smaller events, extending three orders of magnitude in flare fluence were studied by Lenters et al. (2003, see especially their Fig. 13). Their study reveals that the ratio of the fluence of the enhanced X-ray emission $\delta E_{\rm X}$ to the fluence of the preceding burst energy $\delta E_{\rm burst}$ is ~ 0.02, and remains constant from burst to burst. In our models, this ratio can be written as $\gamma = \delta E_{\rm X}/\delta E_{\rm burst} \simeq 2\beta_{\rm b} f(R_{\rm in}/R_*)$ where both $\beta_{\rm b}$ and $R_{\rm in}$ represent the pre burst inner disk conditions. $\beta_{\rm b}$ depends on the disk geometry and is very likely to be similar prior to the different bursts of SGR 1900+14. Our models with a constant f along the X-ray enhancement phase fits well to the data indicating that f remains constant along this phase. Since the X-ray enhancements following the three other smaller events trace accretion rates that were encountered along the decaying tail of the post giant flare enhancement, a similar f must be operating throughout the smaller enhancements following the three events. The remaining variable $R_{\rm in}$ depends on the pre burst $\dot{M}_{\rm in}$. An order of magnitude change in $\dot{M}_{\rm in}$ causes a change in $R_{\rm in}$ by a factor $\lesssim 2$. So, based on our model results, it is understandable that the ratio γ remains constant within a factor ~ 2 for different bursts of a particular SGR, consistent with the observations of SGR 1900+14. γ may vary from source to source depending on the preburst inner disk conditions.

5. Conclusion

We have shown that the X-ray flux curve following the 1998 August 27 giant flare of SGR 1900+14 can be accounted for by the enhanced accretion onto the neutron star surface due to the relaxation of the disk, starting from new initial conditions with the inner disk pushed back by a plausible fraction of the flare energy. For our disk models, the ratio of the fluence of the X-ray enhancement to the preceding burst energy remains roughly constant for bursts of a given SGR with similar preburst mass inflow rates, in agreement with the burst and enhancement observations of SGR 1900+14 (Lenters et al. 2003). This ratio can vary for different SGRs indicating their different inner disk conditions.

We thank Ersin Göğüş and Peter Woods for discussions, and the referee for useful-comments. We acknowledge support from the High Energy Astrophysics Research Group TBAG-Ç-4 of TÜBİTAK and from the Astrophysics and Space Forum at Sabancı University. MAA acknowledges support from the Turkish Academy of Sciences.

REFERENCES

Alpar, M.A. 2001, ApJ, 554, 1245

Chatterjee, P., Hernquist, L., and Narayan, R. 2000, ApJ, 534, 373

Ertan, Ü., and Alpar, M.A., 2002, A&A, 393, 205

Feroci, M., Hurley, K., Duncan, R., and Thompson, C. 2001, ApJ, 549, 1021

Frank, J., King, A.R., and Raine, D., 1992, Accretion Power in Astrophysics (Cambridge: Cambridge University Press)

Hurley, K. et al. 1999, Nature, 379, 41

Hurley, K. 2000 in AIP Conf. Proc. 526, Gamma-Ray Bursts: Fifth Huntsville Symp., ed. R. M. Kippen, R. S. Mallozzi, and G. J. Fishman (New York: AIP), 763

Kaplan, D.L., Kulkarni, S.R., Frail, D.A., and van Kerkwijk, M.H., 2002, ApJ, 566, 378

Lenters, G.T. et al. 2003 (astro-ph 0301577, accepted)

Lyubarsky, Y., Eichler, D., and Thompson, C. ApJ, 580, L69

Mazets, E.P., Cline, T., Aptekar, R.L., Butterworth, P., Frederiks, D.D., Golenetskii, S.V., Il'inskii, V.N., and Pal'shin, V.D.1999, Astron.Lett., 25, 635

Mazets, E.P., Golenetskii, S.V., Il'inskii, V.N., Aptekar, R.L., & Guryan, Y.A. 1979 Nature, 282, 587

Mereghetti, S. 2000, in the Neutron Star-Black Hole Connection, ed. C. Kouveliotou, J. Ventura, and E.P.J. van den Heuvel (Dordrecht:Reidel)

Remillard, R., Smith, D., and Levine, A. 1998, IAU Circ. 7002

Shakura, N.I., and Sunyaev, R.A., 1973, A&A, 24, 337

Thompson, C., and Duncan, C. R. 1995 MNRAS, 275, 255

Thompson, C., and Duncan, C. R., Woods, P.M., Kouveliotou, C., Finger, M.H., and van Paradijs, J. 2000, ApJ, 543, 340

Vrba, F.J., Henden, A.A., Luginbuhl, C.B., Guetter, H.H., Hartmann, D.H., and Klose, S. 2000, ApJ, 543, L17

Woods, P.M., Kouveliotou, C., Göğüş, E., Finger, M.H., Swank, J., Smith, D.A., Hurly, K., and Thompson, C.2001, ApJ, 552, 748

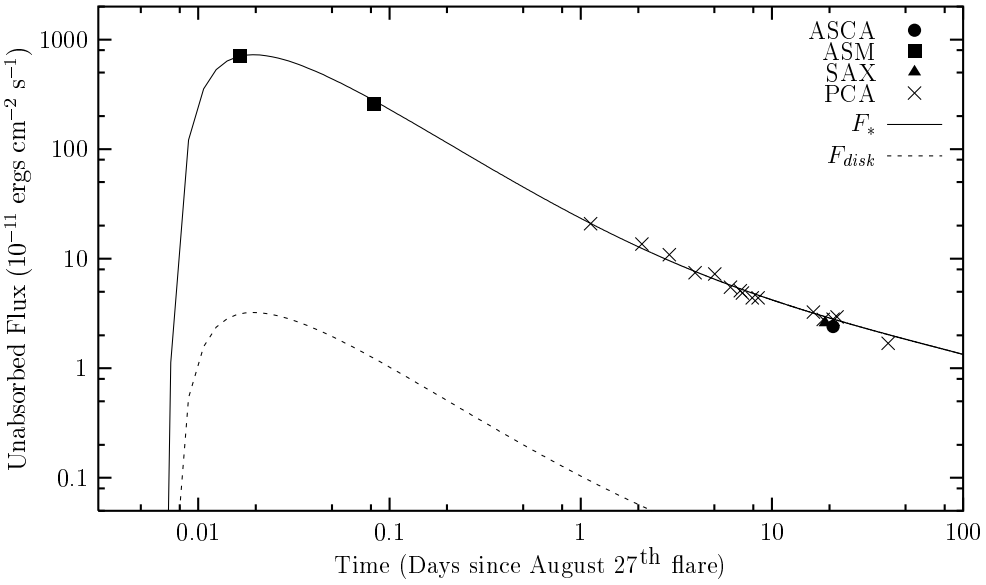

Fig. 1 — The data points (RXTE/ASM, RXTE/PCA, BeppoSAX and ASCA measure

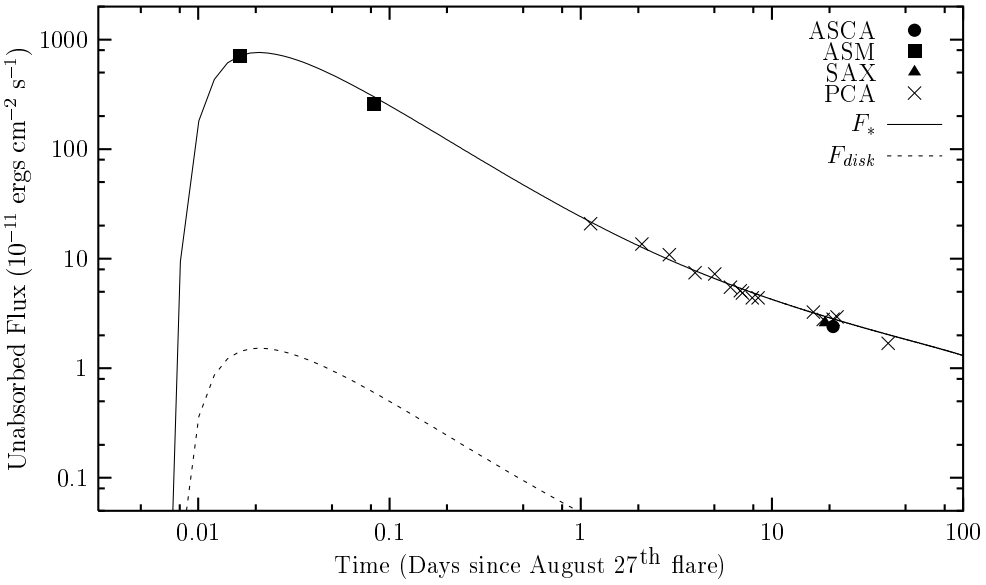

Fig. 2 — Same as Fig. 1 except $f = 0.5$

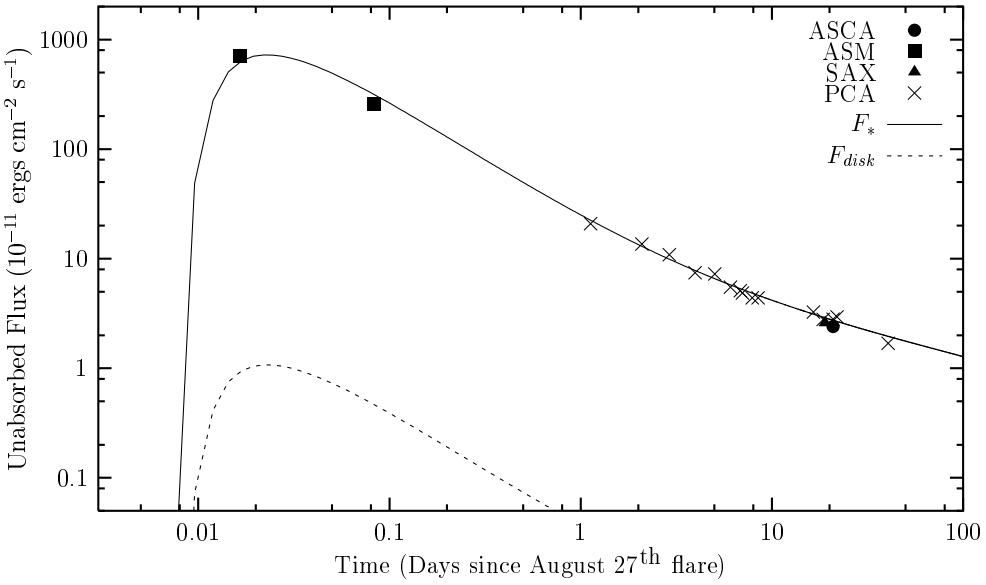

Fig. 3 — Same as Fig. 1 except $f = 0.9$.

Table 1: Model parameters for the flux evolution presented in Fig. 1. In all model calculations, the viscosity parameter $\alpha = 0.1$, the mean molecular weight $\mu = 0.6$ and electron scattering opacities are used

	MODEL 1	MODEL 2	MODEL 3
$\Sigma_{\rm max}$ (g cm^{-2})	9.6×10^4	3.0×10^4	2.1×10^4
Gaussian width (cm)	2.4×10^7	2.2×10^7	2.2×10^7
$\Sigma_0/\Sigma_{\rm max}$	0.012	0.020	0.022
R_0 (cm)	1.8×10^9	1.1×10^9	9.4×10^8
$R_{\rm in}$ (cm)	6.0×10^8	4.0×10^8	3.0×10^8
$R_{\rm out}$ (cm)	1.0×10^{11}	1.0×10^{11}	1.0×10^{11}
f	0.1	0.5	0.9
estimated $\beta_{\rm b}$	2×10^{-4}	5×10^{-5}	4×10^{-5}
δM (g)	2×10^{23}	3.5×10^{22}	2×10^{22}